PLASMA PROCESSES
AND POLYMERS

Bidirectional mass transfer-based generation of plasma-activated water mist with antibacterial properties

Elena V. Sysolyatina[1] | **Aleksandra Y. Lavrikova[2]** | **Roman A. Loleyt[3]** |
Elena V. Vasilieva[1,4] | **Mariam A. Abdulkadieva[4,5]** | **Svetlana A. Ermolaeva[1]** |
Aleksey V. Sofronov[3]

[1]Laboratory of Ecology of Pathogenic Bacteria, N. F. Gamaleya National Research Centre of Epidemiology and Microbiology, Ministry of Health of the Russian Federation, Moscow, Russia

[2]Faculty of Mathematics, Physics and Informatics, Comenius University, Bratislava, Slovakia

[3]KinetikaLab, Moscow, Russia

[4]Department of Dusty Plasma, Joint Institute for High Temperatures, Russian Academy of Sciences, Moscow, Russia

[5]Institute of Biochemical Technology and Nanotechnology, Peoples' Friendship University of Russia, Moscow, Russia

Correspondence
Elena V. Sysolyatina, Laboratory of Ecology of Pathogenic Bacteria, N. F. Gamaleya National Research Centre of Epidemiology and Microbiology, Ministry of Health of the Russian Federation, 18 Gamaleya, Moscow 123098, Russia.
Email: demiurg_84@mail.ru

Abstract

Plasma-activated water mist (PAWM) is obtained by the ignition of plasma within an air–vapor mixture. PAWM demonstrates significant antibacterial properties, decreasing loads of foodborne pathogens by a factor of 35.5 for *Listeria monocytogenes*, 166 for *Salmonella* Typhimurium, and 266 for *Escherichia coli* O157:H7 within 15 s. Bacterial biofilms have a similar species-dependant susceptibility. Biofilms of *L. monocytogenes*, *Salmonella* Typhimurium, and *E. coli* O157:H7 are destroyed by 44%, 77%, and 71%, respectively, after being treated for 2 min. Obtained results suggest importance of short-lived radicals, because PAWM condensate is not bactericidal. A new model of PAW generation as a cyclic process of oxidation reactive nitrogen species by reactive oxygen species, which occurs during effective bidirectional mass transfer between heavily humid air and water mist in plasma discharge, is presented.
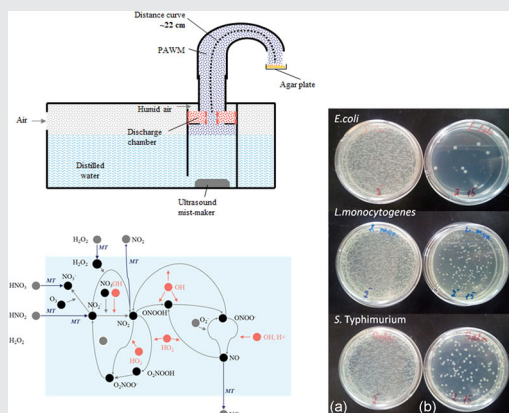
KEYWORDS
bactericidal solution, bidirectional mass transfer, nonthermal plasma, plasma-activated water mist, plasma activation model

1 | INTRODUCTION

Cold atmospheric plasma (CAP) is a promising technology for medicine, sterilization, and surface and water treatment. CAP has bactericidal, fungicidal, and sporicidal effects,[1–4] as well as a selective toxic effect on tumor cells.[5,6] It also stimulates proliferation of keratinocytes[7] and fibroblasts,[8,9] which leads to accelerated wound healing.[10–14] These effects are due to the fact that plasma torch has a large number of active particles at a relatively low concentration, which have a synergistic action.[15,16] There are many approaches of applying CAP to a biological tissue, including (a) direct plasmas, plasma torch and dielectric barrier discharge (DBD), (b) indirect plasmas, plasma is produced between two electrodes and then is transported to area of application, (c) hybrid plasmas, a combination of direct and indirect plasmas, including barrier corona discharge.[17]

It was found that not only CAP has bactericidal properties, but water treated with plasma (plasma-activated water [PAW]) also becomes an effective bactericide solution. The main indicators contributing to the antimicrobial activity of PAW are the accumulation of charged particles in the solution, which leads to a reduction in the pH of distilled water to 3, and the increase in conductivity and redox potential.[18–20] In general, many factors impact the aqueous plasma species that are formed in a solution, including (a) choice of feed gas, (b) construction of the plasma generator and the system power input, (c) solution properties (pH, conductivity, and composition), and (d) time parameters, as discussed in detail below. These parameters can be varied to tailor the resultant solution chemistries for a subsequent therapeutic application.[21]

Due to high oxidation redox potential (ORP) and low pH, PAW has a bactericidal effect and can be used for mild decontamination.[22–24] This usage of PAW is of particular importance for food and beverage industry. The bactericidal effect of PAW depends on the incubation time and type of microorganism: prokaryotes (bacteria) are more susceptible than eukaryotes (fungi).[25–29]

It is important to mention that PAW maintains its antibacterial properties during storage at −80°C over a long time period (30 days), but storage at room temperature decreases its bactericidal effect more than 10 times,[30] probably due to a decrease in nitrite and peroxynitrite concentrations at a stable pH.[31]

There are many different approaches to PAW generation: one is to induce the plasma directly into the water and the second one involves discharges over water and hydrated surfaces[25,32–35] or gas discharge in bubbles.[36] The main disadvantage limiting the use of PAW for decontamination is the long treatment time: It takes 5–30 min on average to achieve a 4–6 log reduction in viability of bacteria.[25,31,32] In all conducted experiments, activated water was added to the bacterial suspension or contaminated objects (plates with adhesive bacteria) were immersed in it. Thus, it is necessary to further drain the objects during the practical application of PAW in food industry, for example, which requires additional labor and time.

Mechanisms of water activation by plasma have been actively discussed in the past few years. Various hypotheses of the antibacterial effect have been suggested, and the main bactericidal molecules have been named, that is, hydrogen peroxide interaction with UV radiation,[37] ozone O_3,[38] HNO_2,[39] and peroxynitrite ONOOH.[40] Liu et al.[41] suggested the hypothesis about the mechanism of reactive nitrogen species (RNS) oxidation with reactive oxygen species (ROS) during PAW generation. This was an important step to further investigate and understand the PAW effects. However, there is still no clear understanding about the mechanism of the PAW bactericidal effect.

Meanwhile, this limited understanding of PAW mechanisms limits its practical implementation. In this study, we have described a novel approach to generation of water-based active media. Plasma-activated water mist (PAWM) was obtained using an original generator by a bidirectional mass transfer between humidified air and water mist. The bactericidal properties of PAWM were proved against foodborne pathogens *Listeria monocytogenes*, *Escherichia coli* O157:H7, and *Salmonella enterica* serovar Typhimurium.

2 | EXPERIMENTAL SECTION

2.1 | Plasma generator and generation of PAWM

The plasma-activating water reactor consists of a tank filled with distilled water, ultrasound mist maker placed at the bottom of the tank, and a discharge chamber. The principal scheme of plasma reactor is shown on Figure 1.

The discharge camera consists of two coaxial quartz tubes (inner and outer) and two electrodes connected to a high-voltage power source (Figure 2a,b). Electrodes are two spirals on which a thin nichrome wire is wrapped (Figure 2b). Electrodes are connected to a high-voltage power source (f, ~15 kHz; amplitude, ~30 kV). Tubes are placed on a horizontal plate that has a number of holes drilled in it. There is an ultrasonic mist maker below the horizontal plate. The outer quartz tube also has a number of drilled holes to ensure airflow.

During the plasma reactor operation, the fan supplies a small amount of air to the tank (about 1.6 cubic feet per minute [CFM]). The air is humidified while passing over the water surface. This humid air enters the discharge

FIGURE 1 The principal scheme of plasma reactor

Air-vapor mixture

Humid air

Air

Discharge chamber

Distilled water

Ultrasound mist-maker
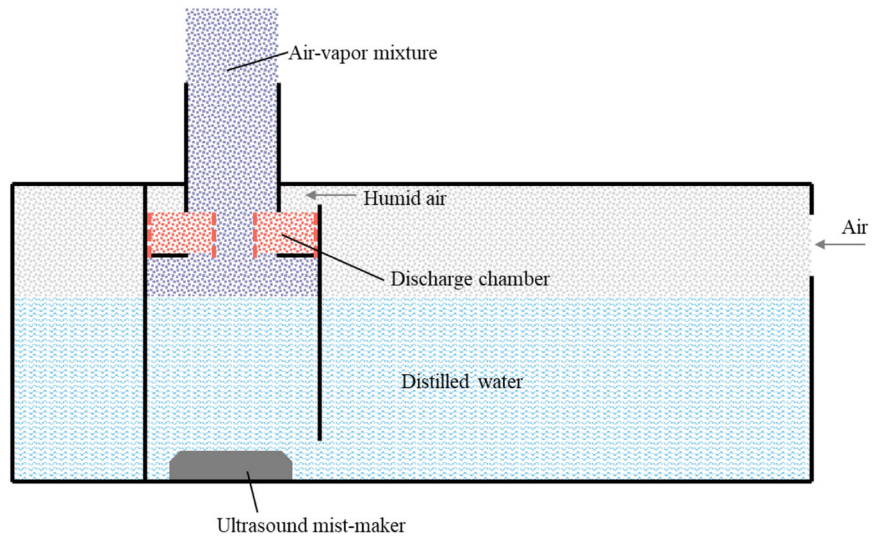
chamber through the holes in the outer tube and passes through DBD. Then the air passes through holes in the horizontal plate and is mixed with the mist from the ultrasonic humidifier, and it enters the inner tube. The air–vapor mixture is retreated by DBD during its movement through the inner tube.

As a result, a plasma-activated air–vapor mixture is obtained. This mixture will be called as PAWM hereinafter.

The liquid that formed on the glass walls of the pre-cooled flask due to the PAWM condensation process will be hereinafter called as a PAWM condensate.

2.2 | Conditions of PAWM treatment and the process of obtaining the PAWM condensate

For PAWM treatment, Petri dishes were inserted into the PAWM at a distance of 22 cm from the discharge chamber (Figure 3a).

For the condensate collection, the pre-cooled flask was used, which was installed on the freezing block (Figure 3b). It took 30 min with three 5-min breaks for obtaining 10 ml of the PAWM condensate.

(a)

V

R_3

d

R_2

R_1

Humid air

Outer electrode

Plasma

Inner electrode

Outer dielectric tube

Air-vapor mixture
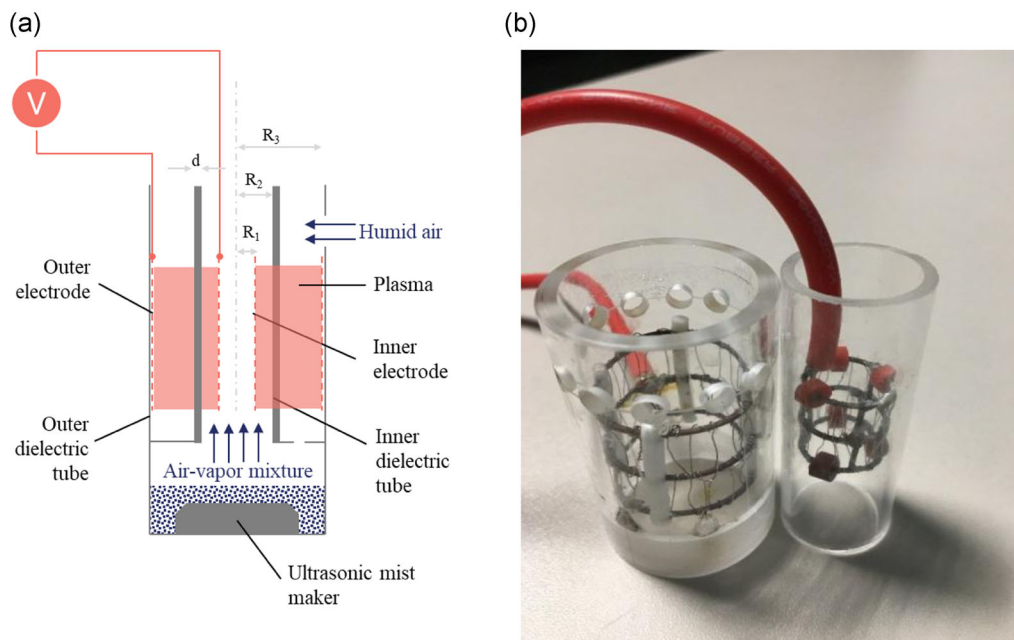
Inner dielectric tube

Ultrasonic mist maker

(b)

FIGURE 2 (a) The design of a discharge chamber ($R_1 = 7$ mm, $R_2 = 9$ mm, $R_3 = 14$ mm). (b) The photo of electrodes of a disassembled discharge camera
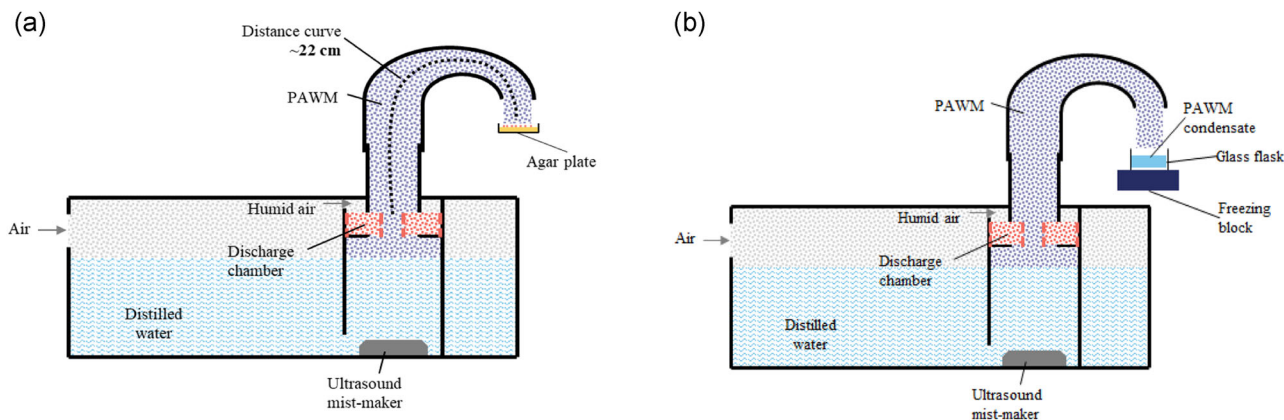
(a)

(b)

FIGURE 3 (a) A scheme of plasma-activated water mist (PAWM) treatment and (b) the process of obtaining the PAWM condensate

2.3 | The quantification of PAWM amount, condensates on agar plate/glass

Petri dishes/glasses were weighted using analytical scales before and after the treatment with PAWM three times to measure the weight of the condensed PAWM. It was established that 15-s treatment of 35-mm Petri dish and the glass led to the settlement of 30 and 20 µl of the PAWM condensate, respectively.

2.4 | Bacterial strains

Bactericidal effects were tested on pathogenic bacteria from the Gamaleya Research Centre collection, the Gram-negative enterohemorrhagic *E. coli* O157:H7 strain ATCC43890 (EHEC), the *Salmonella enterica* serovar Typhimurium strain IE147, and the Gram-positive *L. monocytogenes* (the EGDe strain). *E. coli* and *S.* Typhimurium were grown on Luria Bertani Agar (Amresco), *L. monocytogenes* was cultivated on Brain Heart Infusion Agar (BD) at 37°C.

2.5 | The bactericidal effect of PAWM and PAWM condensate on planktonic bacteria

For the evaluation of the bactericidal effect of PAWM, decimal dilutions of the overnight bacterial culture were plated on 35-mm agar plates and treated with PAWM for 5, 10, 15, and 30 s. The vapor was uniformly distributed over the Petri dish. Experiments were performed in triplicate and repeated three times for every bacterial strain.

The antibacterial effect of PAWM condensate was tested by adding the appropriate amount of PAWM condensate onto Petri dishes with preseeded bacteria.

The bacteria were plated onto agar and in 5 min 30 µl of PAWM condensate was added.

The viability of bacteria after PAWM or PAWM condensate treatment was evaluated after 24 hr of incubation at 37°C by the colony counting method and compared with the untreated control.

2.6 | Live/Dead staining of planktonic bacteria

To evaluate the level of the bacterial membrane integrity immediately after treatment, Live/Dead staining of *E. coli* O157:H7 bacteria was performed within 1–2 min after treatment as follows.

30 µl of bacterial suspension with the initial concentration of 1×10^7 CFU/ml was spread over the piece of glass. When the drop was dried at room temperature, the bacteria that remained on the surface were treated for 15 s and immediately stained afterward by Live/Dead Kit (Invitrogen) to distinguish the "living" bacteria with undamaged membranes (green) from the "dead" ones (red). The staining was performed in accordance with the manufacturer's instruction. Untreated bacteria were used as a control. The pictures were obtained with Zeiss AxioVision microscope and multiplication of ×1,000

2.7 | The effect of PAWM and PAWM condensate on biofilms

150-µl *E. coli*, *Salmonella* Typhimurium, or *L. monocytogenes* at initial concentrations of 10^7 cells/ml were seeded into the wells of a 96-well plate. Bacteria were incubated for 72 hr at 37°C without shaking. Afterward, the wells were rinsed three times with 200 µl of sterile phosphate-buffered saline (PBS) and treated for 2 and 5 min

TABLE 1 Characteristics of PAWM condensate in comparison with distilled water

	Distilled water	PAWM condensate
pH	6.4 ± 0.1	2.3 ± 0.1
ORP	170 ± 5	560 ± 5
Conductivity	13.0 ± 0.3	$2,730 \pm 55$

Abbreviations: ORP, oxidation redox potential; PAWM, plasma-activated water mist.

with PAWM or were filled with 150-μl PAWM condensate for 2 and 5 min. Then the surplus of liquid was removed and the wells were filled with 140 μl of 0.1% crystal violet (water solution). After 15 min, the crystal violet was removed and the wells were rinsed three times with PBS and left for 15 min upside down for drying. After this, 140 μl of 96% ethanol was added in each well. The suspension was mixed and incubated at room temperature for 15 min. Then, the optical density of the solution was measured at

FIGURE 4 Petri dishes with plasma-activated water mist-treated bacteria (a) control, (b) 15-s treatment

590 nm (OD_{590}) with the an iMark Microplate Reader (BioRad). Untreated wells were used as a control.

3 | RESULTS

The PAWM generator is described in detail in Section 2 and shown in Figures 1 and 2a,b. The overall operating principle is as follows: Water mist is generated by the piezoelectric ceramic, humidified air passes through the DBD and is mixed with the water mist, and then the air–mist mixture again passes through the DBD. As a result, the PAWM is obtained.

3.1 | Acidizing water mist in DBD

To measure pH, ORP, and conductivity, PAWM was collected by the condensing mist in a glass flask. It took about 30 min of operation to collect the required amount of condensate (5 ml). Before treatment, the pH of sterile deionized water was in the range of 6.30–6.55. In general, as a result of PAW generation in water, the pH decreased from neutral to acid, that is, from 6.4 ± 0.1 to 2.3 ± 0.1. ORP increased from 170 to 560 mV. Conductivity increased from 13 to 2,730 μS (Table 1). Electrochemical changes of PAWM condensate were not unexpected and were demonstrated in many studies.[26,27,29] Acidizing of water and the increase of ORP and conductivity can be explained by the accumulation of plasma-chemical reaction products in water (specifically HNO_2, HNO_3, H_2O_2, and HO_2).

To avoid overheating the samples, we measured the PAWM temperature. The PAWM temperature was 32°C at the working distance, and therefore it was permissible for bacteria.

The pH of the PAW remained constant during the storage for a period of 7 days (data are not shown).

3.2 | PAWM provided the maximum antibacterial effect after 15 s of treatment

The bactericidal effect of PAWM was tested on bacteria that cause foodborne infections: *E. coli* O157:H7 (EHEC; hemorrhagic colitis), *L. monocytogenes EGDE* (listeriosis), and *Salmonella* Typhimurium (salmonellosis). Bacteria were seeded into Petri dishes and were treated with the mist for 5, 10, 15, and 30 s.

All three species were susceptible to PAWM treatment (Figure 4). Even a 5-s treatment was bactericidal, causing a 9.2-, 5.9-, and 3.1-fold decrease for *L. monocytogenes, E. coli* O157:H7, and *Salmonella* Typhimurium, respectively
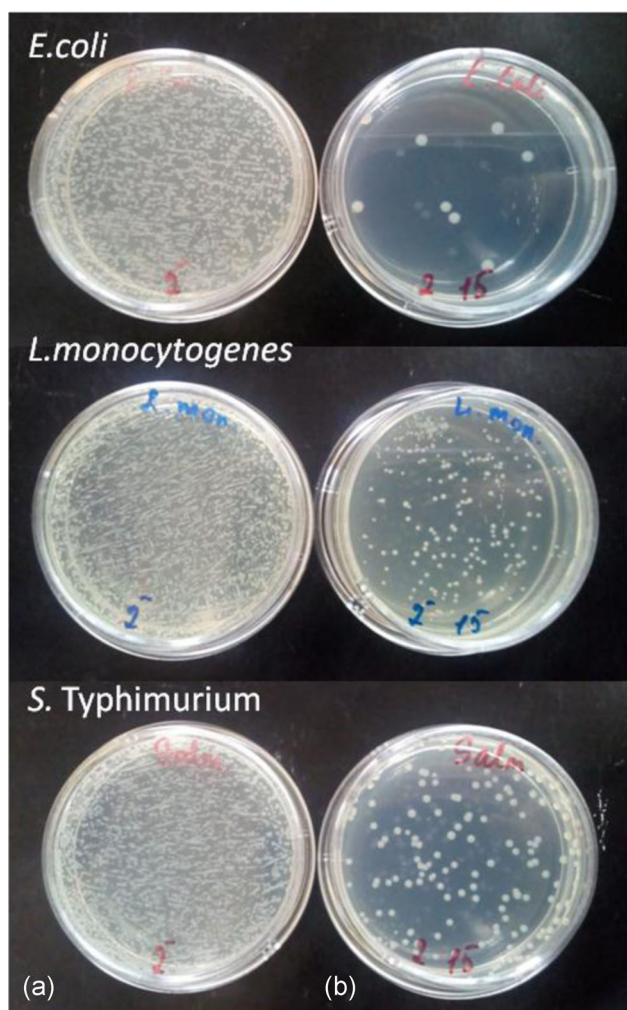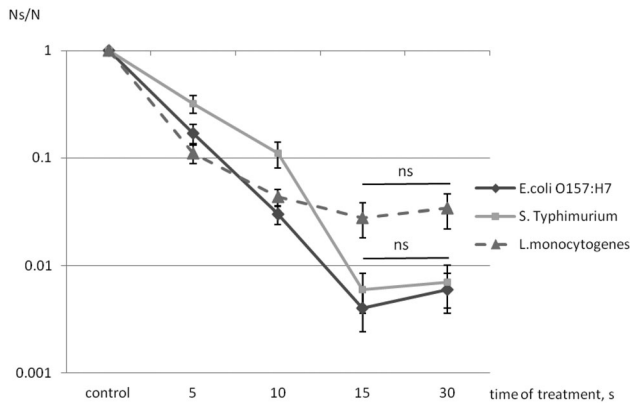
FIGURE 5 The time-dependent bactericidal effect of plasma-activated water mist. N, the amount of bacteria in a control group; Ns, the amount of survived bacteria; ns, $p > .05$

$(p < .05$; Figure 5). The increase of treatment time to 10 and 15 s caused a further reduction in bacterial viability. The maximal bactericidal effect was obtained after the 15-s treatment. Unlike during the 5-s PAWM application, *L. monocytogenes* had the least susceptibility: The amount of survived bacteria decreased by a factor of 35.5. *E. coli* O157:H7 was the most susceptible and *Salmonella* Typhimurium had a medium result: The bacterial load decreased by a factor 266 and 166.2, respectively (Figure 5). It is interesting that the bacterial species demonstrated a different dependence on the treatment time, with *L. monocytogenes* demonstrating the least difference between treatment for 10 and 15 s (Figure 5). Extending treatment duration to 30 s did not cause reliable changes in bactericidal effect for all species ($p > .05$).

Thus, it was established that the bactericidal effect of PAWM was dose-dependent and reached its peak after 15 s of treatment. It was 35.5 for *L. monocytogenes*, 166 for *Salmonella* Typhimurium, and 266 times for *E. coli* O157:H7. The PAWM efficacy highly depended on the microbial

species. *L. monocytogenes* exhibited a less susceptibility to PAWM, compared with *Salmonella* Typhimurium, which is in accordance with the study of Smet et al.[32] It should be also noticed that the bactericidal effect of PAWM may be limited. However, mechanisms underlying these limits are not clear yet. It is not clear now if this limit has biological nature (due to the individual nongenetic resistance of bacteria) or is associated with the inability of PAWM to penetrate some microcavities of the agar surface.

3.3 | PAWM treatment immediately damages the membrane of bacteria

To test if the bacteria damage after PAWM treatment was immediate or the bactericidal effect was due to a delayed process of the interaction of bacteria with a layer of PAWM on the agar surface, the Live/Dead staining was conducted right after the PAW treatment. As the highest bactericidal effect was achieved for *E. coli* O157:H7 after 15-s treatment, we used these conditions to established if such significant reduction of bacterial load (by 266 times) was due to immediate damaging of bacteria or not.

Bacteria dried on the glass surface, as described in Section 2, were treated by PAWM for 15 s. Then, bacteria were immediately stained with the Live/Dead dye (Figure 6). Before PAWM treatment, the majority of the cells attached to the glass surface were live (green), but after 15 s of treatment, we observed cell detachment and membrane damage (red staining). The experimental data we obtained support the hypothesis that the damage of bacterial cells occurs during or immediately after the PAWM contact.

Thus, PAWM had a significant and instantaneous antibacterial effect on foodborne pathogens just after 10–15 s of treatment.
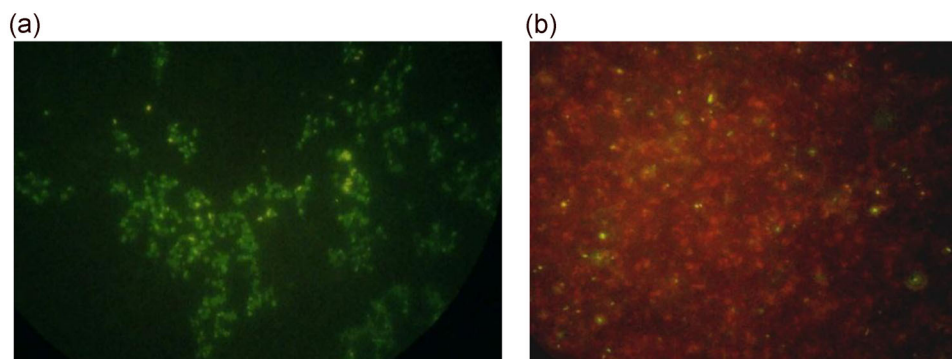

FIGURE 6 The effect of plasma-activated water mist on *Escherichia coli* O157:H7 membrane integrity. (a) Untreated control, (b) 15-s treatment. Green, "live" bacteria; red, "dead"

TABLE 2 The bactericidal effect of PAWM condensate

Bacterial species	Ns/N
Listeria monocytogenes	1.07 ± 0.15
Escherichia coli O157:H7	0.8 ± 0.1
Salmonella Typhimurium	0.31 ± 0.07*

Abbreviations: N, the amount of bacteria in a control group; Ns, the amount of survived bacteria; PAWM, plasma-activated water mist.

*$p < .05$.

3.4 | PAWM condensate has weak bactericidal properties

It was established that during the 30-s PAWM treatment, 30 μl of condensate settled on an agar plate. To test the bactericidal effect of PAWM condensate alone, we added 30 μl of the previously obtained condensate to the agar surface with preseeded bacteria. This amount of condensate was not bactericidal for *L. monocytogenes* and *E. coli* O157:H7, and it decreased bacterial loads by a factor of 3 for *Salmonella* Typhimurium ($p < .05$; Table 2).

3.5 | Two-minute PAWM treatment destroys biofilm matrix

72-hr biofilms of *E. coli* O157:H7, *Salmonella* Typhimurium, and *L. monocytogenes* were treated with PAWM for a period of 2 and 5 min. After this, they were stained with 0.1% crystal violet to estimate the amount of remaining biofilm matrix. We used untreated samples as a control.
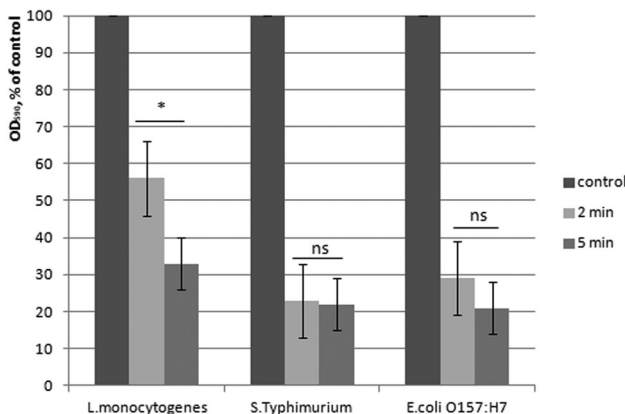
The antibiofilm effect of PAWM was species-dependent and corresponded to the bactericidal effect to planktonic cells. The most susceptible was the biofilm of *E. coli* O157:H7: After 2 min of PAWM, the biofilm biomass evaluated with the crystal violet staining decreased up to 71% ($p < .01$; Figure 7). This effect was maximal, and the prolongation of treatment to 5 min did not enhance the antibiofilm properties of PAWM ($p > .05$).

Salmonella Typhimurium biofilm had a similar susceptibility: After 2 min of PAWM, its biomass decreased by up to 77% ($p < .01$; Figure 7). The differences between groups treated for 2 and 5 min were not statistically significant ($p > .05$). The five-minute treatment did not cause an increase in the antibiofilm effect.

The biofilm of *L. monocytogenes* had the highest resistance to PAWM: After 2 min of its application, *L. monocytogenes* biofilm biomass decreased by up to 44%. This effect was time-dependant: The increase in the treatment duration to 5 min enhanced the antibiofilm effect by up to 67% ($p < .05$).

So, the biofilms formed by *Salmonella* Typhimurium and *E. coli* O157:H7 were more susceptible to PAWM than the biofilm of *L. monocytogenes*. The decrease in the biofilm biomass suggested that PAWM destroyed the bacterial biofilms.

3.6 | PAWM condensate has a similar antibiofilm effect

The antibiofilm effect of the PAWM condensate also was species-dependent. The biofilm of *L. monocytogenes* had the highest resistance to PAWM condensate, and after 2 min of application, the biofilm biomass decreased by up to 52% (Figure 8) It was similar to the effect of PAWM (44%),
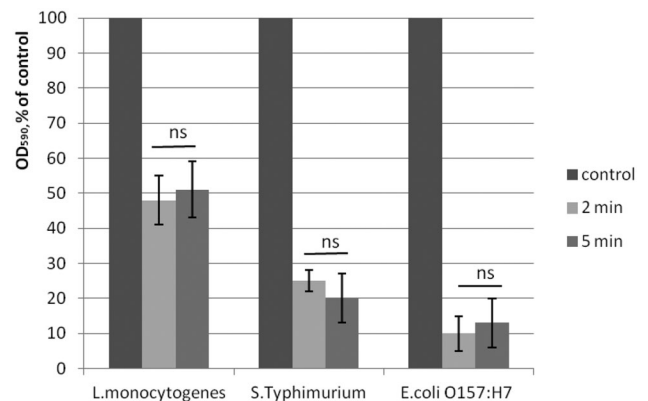
FIGURE 7 Relative changes of optical density (OD) of crystal violet after plasma-activated water mist treatment of biofilms of *Listeria monocytogenes*, *Salmonella* Typhimurium, and *Escherichia coli*; ns, $p > .05$; *$p < .05$

FIGURE 8 Relative changes of optical density (OD) of crystal violet after plasma-activated water mist condensate treatment of biofilms of *Listeria monocytogenes*, *Salmonella* Typhimurium, and *Escherichia coli*; ns, $p > .05$

and this difference was not statistically sufficient ($p > .05$). The increase in the treatment duration to 5 min did not increase the rate of biofilm destruction.

Salmonella Typhimurium biofilm had a medium susceptibility: After 2 min of PAWM condensate application, the biofilm biomass decreased by up to 75% ($p < .01$) (Figure 8). The five-minute treatment did not enhance the effect. The differences between experimental groups were not statistically significant ($p > .05$).

The *E. coli* O157:H7 biofilm was the most susceptible: After applying PAWM condensate for 2 min, its biomass decreased by up to 90% from 1 to 0.1 c.u. ($p < .01$; Figure 8). This effect was higher in comparison with the effect of PAWM, 71%, but the increase of the treatment duration to 5 min did not enhance the antibiofilm properties of the condensate.

So, the biofilms formed by *Salmonella* Typhimurium and *E. coli* O157:H7 were more susceptible to PAWM disintegration than the biofilm of *L. monocytogenes*, as it was established for the planktonic cells previously. However, unlike the planktonic cells, we did not observe any statistically significant differences between PAWM and PAWM condensate antibiofilm effect.

4 | DISCUSSION

Plasma discharges over the water surface as well as discharges directly in water proved to neutralize a wide range of microorganisms. In some cases, PAW has proven to be more effective than direct plasma treatment. For example, CAP and PAW were used to treat strawberries contaminated with *Staphylococcus aureus*.[23] Direct plasma treatment of the strawberries over a period of 15 min caused 1.72 log10 CFU/ml reduction of the bacterial load. The exposure of the contaminated strawberries to PAW for 20 min reduced the bacterial load by up to 3.5 log10 CFU/ml.[23]

On the one hand, the bactericidal effect of PAW depends on the morphology and physiology of bacterial species. Gram-negative bacteria usually are more susceptible to direct plasma treatment and to PAW application.[32,36,42–44] On the other hand, the antibacterial properties of PAW are linked to electrophysical parameters of plasma generator and ongoing chemical processes in plasma-treated liquids. It is supposed that the formation of ROS and RNS in PAW and their interactions with cellular components like cell membrane and wall, nucleic acids, and internal proteins are responsible for the microbial cell inactivation.[45]

NO, which is present in the plasma area that is directly above the water, can be easily oxidized to NO_2. These radicals can consequently produce NO_2^- and NO_3^- in the water.[46] At a low pH,[39] the nitrous acid that is also

formed is not stable and it decomposes rapidly into nitrogen dioxide. If this nitrogen dioxide reacts with hydroxyl radicals, peroxynitrous acid is formed, subsequently converting into nitrate. In addition, if NO_2^- reacts with H_2O_2 under acidic conditions, nitrate can also form.[40] Thus, according to chemical and electrochemical characteristics of PAW, it is a liquid solution of RONS with a high redox potential and low pH.

It was established that regardless of the type of microorganisms or cell mode, an increase in plasma-activated liquids (PAL) age reduced its microbial inactivation efficacy.[32] The authors[32] made a conclusion that despite the fact that "during storage the concentrations of the important long-lived species remained constant...these findings could again indicate the importance of short-lived species within PAL solutions."

Our experiments showed that PAWM immediately killed bacteria after 15 s of application. The bacterial load decreased from 35.5 times for *L. monocytogenes* to 166 times for *Salmonella* Typhimurium and 266 times for *E. coli* O157:H7. However, the PAWM condensate was not bactericidal for *L. monocytogenes* and *E. coli* O157:H7, and it reduced the bacterial load for *Salmonella* Typhimurium by up to three times. This result is in accordance with the statement that short-living particles can be responsible for the fast bactericidal effect of PAW.[32]

It was established that PAW treatment destroyed the dimensional structure and normal morphology of the biofilm of *Enterococcus faecalis*,[47] but the mechanism of action was not clear. Later, Zhou et al.[48] demonstrated that both air microplasma bubbles and PAW reduced the existing biofilm of *E. coli* load by ~83% and 60%, respectively, after 15 min of discharge.[48] They proposed that the main role in the biofilm destruction was to draw a balance between NO and other ROS and NOS. Such nitrogen species, as peroxynitrite and dinitrogen trioxide, may interact with matrix components (extracellular DNA and polysaccharides), dissolved solutes in the hydrated matrix of the biofilm, increasing the penetration of the plasma-active species into the biofilm matrix and accelerating its dispersal.

As far as PAWM is a mixture of short- and long-living particles, reacting with each other, we extended the scope of our models to biofilms and treated them during 2 and 5 min. Surprisingly, the antibiofilm effect of PAWM and its condensate was similar. We assumed that a layer of condensed mist that formed during 2-min PAWM treatment on the surface of the wells could have protected the biofilm from the action of new portions of PAWM with short-living particles. Thus, we detected the antibiofilm effect of long-living particles in both cases: after treatment of PAWM and PAWM condensate. Another explanation could be that biofilm shell was naturally more

resistant to RONS. Especially, long-living RONS played a key role in biofilm destruction, whereas short-living RONS could not damage polysaccharide shell during its lifetime. However, these hypotheses required further investigation and experimental proof.

This difference between the bactericidal effect of PAWM and low antibacterial properties of its condensate should be discussed and explained. We suppose that the PAW action mechanism strongly depends on the presence of excited state of oxygen $O(^1D)$, high concentration of H_2O molecules in gas phase, and effective mass transfer between gas and liquid phases.

4.1 | PAWM model: Process of cyclic RNS oxidation

The experimental setup, discussed in previous section, is based on the ignition of plasma in air–vapor mixture. This mixture consists of water droplets with 20–70 microns diameter surrounded by humid air with relative humidity close to 100%. The temperature in the discharge chamber reaches 70–80°C, which means that the concentration of vapor is ~230 g/m³ and gas mixture is 55% N_2:12% O_2:38% H_2O. A significant amount of H_2O in gas phase is critical for plasma chemistry.
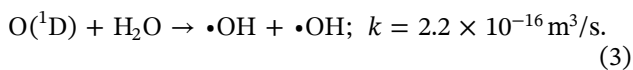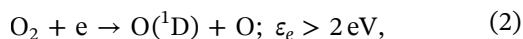
Basic plasma reactions in humid air were previously considered by Akishev,[49] and Julak,[50] Sakyama,[51] The generation of exited states of atomic oxygen $O(^1D)$, hydroxyl radicals OH, hydroperoxyl HO_2, and nitrous acid HNO_2[49–51] was predicted. Basic models of plasma chemistry have been discussed in many studies[41,49–52] over the recent years. In our work, we will not repeat the complete chain of reactions but will instead focus on the points for activation of water droplets that are critically important. It should be noticed that all reaction rates are calculated at a temperature of T ~70°C (343 K).

As mentioned above, plasma discharge was ignited in heavy humid air with water concentration of ~38%. This is a very important condition, as an increase in H_2O concentration in the gas phase accelerates the generation of OH, HO_2, and HNO_2.
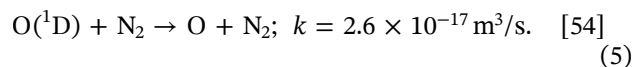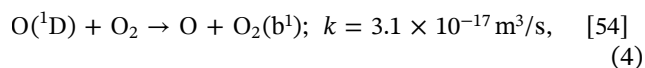
OH radicals can be generated by dissociative electron attachment

$$H_2O + e \rightarrow H^- + \bullet OH; \ \varepsilon_e > 6 \ eV, \tag{1}$$
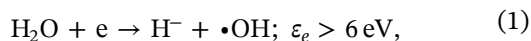
or in reaction of $O(^1D)$ with water molecules

$$O_2 + e \rightarrow O(^1D) + O; \ \varepsilon_e > 2 \ eV, \tag{2}$$

$$O(^1D) + H_2O \rightarrow \bullet OH + \bullet OH; \ k = 2.2 \times 10^{-16} \ m^3/s. \tag{3}$$

DAE (1) is a highly resonant reaction and requires electron energy in a range of 6–8 eV, which is hard to reach in DBD in air with typical electron energy of 1–3 eV. Thus, only the reaction chain (2) and (3) is the most efficient mechanism of OH radical generation. The generation of $O(^1D)$ in reaction (2) requires a relatively low electron energy and it is the major dissociation reaction in gas discharge in air with electron energy > 2 eV.[53] However, reaction (3) in dry air $O(^1D)$ has strong competitors: (4, 5)–deactivation $O(^1D)$ by neutral molecules O_2 and N_2

$$O(^1D) + O_2 \rightarrow O + O_2(b^1); \ k = 3.1 \times 10^{-17} \ m^3/s, \quad [54] \tag{4}$$

$$O(^1D) + N_2 \rightarrow O + N_2; \ k = 2.6 \times 10^{-17} \ m^3/s. \quad [54] \tag{5}$$

The good news is that reaction (3) is 10 times faster than reactions (4, 5), and in humid air, most of the $O(^1D)$ atoms react with H_2O and generate OH radicals. For example, ~90% of $O(^1D)$ reactivates via reactions (4, 5) in dry air with 1% of H_2O and only ~10% generates OH, but in heavily humid air with 38% H_2O, ~75% of $O(^1D)$ generates OH radicals and ~25% gets deactivated. In other words, a high concentration of H_2O in the air is the trigger that shifts reactions with $O(^1D)$ toward the synthesis of OH.

OH radicals are very important as a precursor of HNO_2 due to reaction with NO. NO generation in non-thermal atmospheric pressure plasma in the air has been discussed and proved in many studies.[41,52,55]

$$\bullet NO + \bullet OH + M \rightarrow HNO_2 + M; \ k \\ = 5.4 \times 10^{-43} \ m^3/s. \quad [54] \tag{6}$$
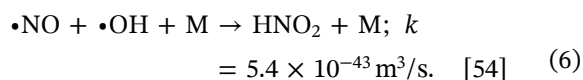
OH radical also reacts with ozone, generating a more stable HO_2 radical

$$\bullet OH + O_3 \rightarrow HO_2 \bullet + O_2; \ k = 8.7 \times 10^{-20} \ m^3/s. \quad [56] \tag{7}$$
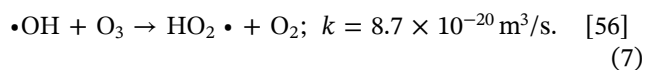
Reaction (7) is not very fast in a near-room temperature, but it can occur near the streamer zone due to local high temperature and high concentration of O_3.

Thus, DBD in heavily humid air accelerates the generation of OH, HNO_2, and HO_2.

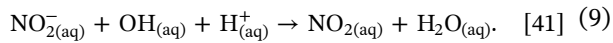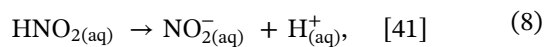Liu et al.[41] considered the mechanism of RNS oxidation by ROS in the liquid phase. Mass transfer between gas and liquid should be considered in line with solubility.[57] RONS Henry's law constants are shown in Table 3.

Direct mass transfer of RNS (NO_x) to the liquid phase is not significant due to its low solubility. Transfer of NO_2 to its liquid phase goes through HNO_2

TABLE 3 Henry's law constants

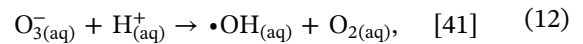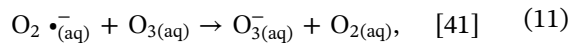| RONS	h
$HO_2\bullet$	1.3×10^5
$\bullet OH$	620
$\bullet NO$	4.4×10^{-2}
NO_2	0.3
$NO_3\bullet$	42
HNO_2	1.2×10^3
H_2O_2	1.9×10^6

Abbreviation: RONS, reactive oxygen and nitrogen species.

$$HNO_{2(aq)} \rightarrow NO^-_{2(aq)} + H^+_{(aq)}, \quad [41] \quad (8)$$

$$NO^-_{2(aq)} + OH_{(aq)} + H^+_{(aq)} \rightarrow NO_{2(aq)} + H_2O_{(aq)}. \quad [41] \quad (9)$$
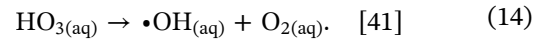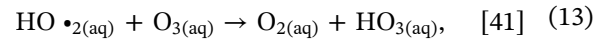
The solubility of OH is also relatively low and mass transfer requires a large area of contact between gas and liquid, which is ensured by large number of small droplets in discharge chamber sized 30–70 microns in diameter.

In addition to the direct transfer of OH radicals, there is also an extra mechanism of OH generation in liquid.

The following is the mechanism of HO_2 reaction with ozone

$$HO_2\bullet_{(aq)} \rightarrow O_2\bullet^-_{(aq)} + H^+_{(aq)}, \quad [41] \quad (10)$$

$$O_2\bullet^-_{(aq)} + O_{3(aq)} \rightarrow O^-_{3(aq)} + O_{2(aq)}, \quad [41] \quad (11)$$

$$O^-_{3(aq)} + H^+_{(aq)} \rightarrow \bullet OH_{(aq)} + O_{2(aq)}, \quad [41] \quad (12)$$

and

$$HO\bullet_{2(aq)} + O_{3(aq)} \rightarrow O_{2(aq)} + HO_{3(aq)}, \quad [41] \quad (13)$$

$$HO_{3(aq)} \rightarrow \bullet OH_{(aq)} + O_{2(aq)}. \quad [41] \quad (14)$$
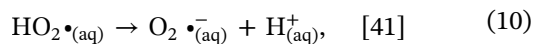
Thus, liquid droplets accumulate NO_2, NO_2^-, OH, and HO_2, and they trigger cyclic oxidation reactions with synthesis and decay of $ONOO^-/ONOOH$ and O_2NOO^-/O_2NOOH[29]:
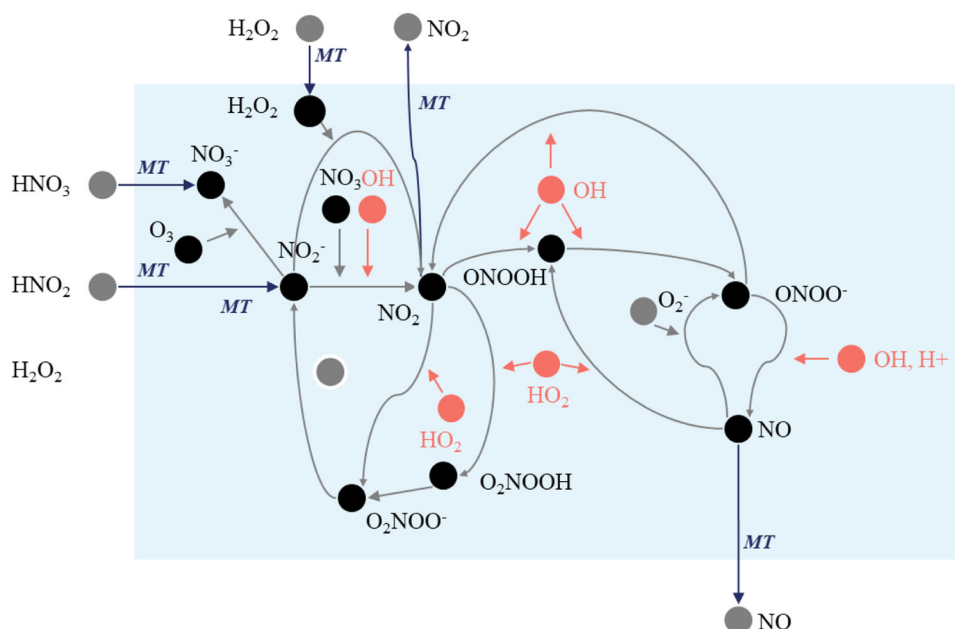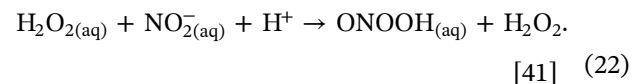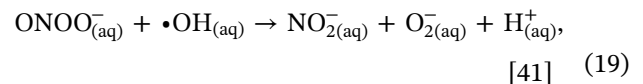
First chain:

$$NO_{2(aq)} + \bullet OH_{(aq)} \rightarrow ONOOH_{(aq)}, \quad [41] \quad (15)$$

$$ONOOH_{(aq)} \rightarrow ONOO^-_{(aq)} + H^+_{(aq)}, \quad [41] \quad (16)$$

$$ONOOH_{(aq)} \rightarrow NO^-_{3(aq)} + H^+_{(aq)}, \quad [41] \quad (17)$$

$$ONOO^-_{(aq)} + \bullet OH_{(aq)} + H^+_{(aq)} \rightarrow \bullet NO_{(aq)} + O_{2(aq)} + H_2O_{(aq)}, \quad [41] \quad (18)$$

$$ONOO^-_{(aq)} + \bullet OH_{(aq)} \rightarrow NO^-_{2(aq)} + O^-_{2(aq)} + H^+_{(aq)}, \quad [41] \quad (19)$$

$$\bullet NO_{(aq)} + HO_2\bullet_{(aq)} \rightarrow ONOOH, \quad [41] \quad (20)$$

$$\bullet NO_{(aq)} + O_2\bullet^-_{(aq)} \rightarrow ONOO^-_{(aq)}, \quad [41] \quad (21)$$

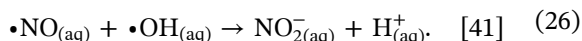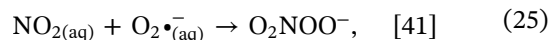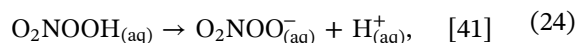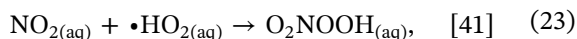$$H_2O_{2(aq)} + NO^-_{2(aq)} + H^+ \rightarrow ONOOH_{(aq)} + H_2O_2. \quad [41] \quad (22)$$
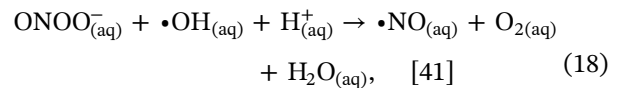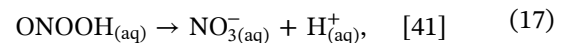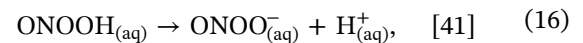
FIGURE 9 A diagram of RNS oxidation in the liquid phase. MT, mass transfer; RNS, reactive nitrogen species

Second chain:

$$NO_{2(aq)} + \cdot HO_{2(aq)} \rightarrow O_2NOOH_{(aq)}, \quad [41] \quad (23)$$

$$O_2NOOH_{(aq)} \rightarrow O_2NOO^-_{(aq)} + H^+_{(aq)}, \quad [41] \quad (24)$$

$$NO_{2(aq)} + O_2\cdot^-_{(aq)} \rightarrow O_2NOO^-, \quad [41] \quad (25)$$

$$\cdot NO_{(aq)} + \cdot OH_{(aq)} \rightarrow NO^-_{2(aq)} + H^+_{(aq)}. \quad [41] \quad (26)$$

The importance of these chains is that they are cyclic (Figure 9)—they consume OH/HO$_2$ as "fuel" and repeat while OH/HO$_2$ is still available.

This oxidation cycle leads us to a novel understanding of PAW. PAW is not just a mix of radicals, but it is a cyclic process of oxidation of NO$_2^-$ by OH and HO$_2$. This process refers to recurrent reaction chains of synthesis and decay of ONOOH and ON$_2$OOH, which consumes OH and HO$_2$ radicals as "fuel." When the "fuel" runs out, the process stops and leaves a tail of NO$_2^-$/NO$_3^-$, NO$_2$, and NO. NO$_2$ and NO have a low solubility and leave liquid water to the gas phase. The PAW process required an effective mass transfer of HNO$_2$, OH, and HO$_2$ from the gas to liquid phase. The easiest way to achieve effective mass transfer is to ignite plasma discharge in water mist. The generation of HNO$_2$, OH, and HO$_2$ accelerates in humid air, that is, the concentration of H$_2$O molecules in the gas phase is high.

5 | CONCLUSION

Bactericide properties of plasma-activated water can be significantly improved by effective mass transfer between gas and liquid phases as well as by increasing energy of free electrons in plasma. The analysis of chemical reactions in the liquid phase led us to a novel understanding of PAW mechanisms. PAW is a cyclic process of chemical reactions between RNS (NO$_2$) and ROS (OH, HO$_2$) with synthesis and decay of ONOO$^-$/ONOOH and O$_2$NOO/O$_2$OOH. This process requires an effective bidirectional mass transfer between gas and liquid phases.

CONFLICT OF INTERESTS
Alexey V. Sofronov is the CEO and Founder of KinetikaLab, owner of technology patent disclosed in publication. Roman A. Loleyt is an employee of KinetikaLab.

ORCID
Elena V. Sysolyatina http://orcid.org/0000-0002-1168-4159

REFERENCES

[1] *Plasma for Bio-Decontamination, Medicine and Food Security, NATO Science for Peace and Security Series A Chemistry and Biology* (Eds: Z. Machala, K. Hensel, Y. Akishev), Springer, New York, NY **2012**.

[2] F. Rossi, O. Kylian, H. Rauscher, D. Gilliland, L. Sirghi, *Pure Appl. Chem.* **2008**, *80*, 1939.

[3] K. Stapelmann, M. Fiebrandt, M. Raguse, P. Awakowicz, G. Reitz, R. Moeller, *Astrobiology* **2013**, *13*, 597.

[4] A. Sakudo, Y. Yagyu, T. Onodera, *Int. J. Mol. Sci.* **2019**, *20*, 5216.

[5] G. Bauer, D. Sersenová, D. Graves, Z. Machala, *Sci. Rep.* **2019**, *9*, 1.

[6] M. Keidar, D. Yan, I. Beilis, B. Trink, J. Sherman, *Trends Biotechnol.* **2018**, *36*, 586.

[7] A. Schmidt, S. Bekeschus, K. Jarick, S. Hasse, T. Von Woedtke, K. Wende, *Oxid. Med. Cell Longevity* **2019**, *2019*, 1.

[8] S. Arndt, P. Unger, E. Wacker, T. Shimizu, J. Heinlin, Y. Li, H. Thomas, G. Morfill, J. Zimmermann, A. Bosserhoff, S. Karrer, *PLOS One* **2013**, *12*, e79325.

[9] E. Sysolyatina, M. Vasiliev, M. Kurnaeva, I. Kornienko, O. Petrov, V. Fortov, A. Gintsburg, E. Petersen, S. Ermolaeva, *J. Phys. D: Appl. Phys.* **2016**, *49*, 294002.

[10] G. Isbary, J. Heinlin, T. Shimizu, Y. Zimmermann, G. Morfill, H. Schmidt, R. Monetti, B. Steffes, W. Bunk, Y. Li, T. Klampfl, S. Karrer, M. Landthaler, W. Stoltz, *Br. J. Dermatol.* **2012**, *167*, 404.

[11] M. Chatraie, G. Torkaman, M. Khani, H. Salehi, B. Shokri, *Sci. Rep.* **2018**, *8*, 1.

[12] A. Nishijima, T. Fujimoto, T. Hirata, J. Nishijima, *Mod. Trends Plast. Surg.* **2019**, *9*, 18.

[13] B. Haertel, T. von Woedtke, K.-D. Weltmann, U. Lindequist, *Biomol. Ther.* **2014**, *22*, 477.

[14] G. Isbary, J. L. Zimmermann, T. Shimizu, Y.-F. Li, G. E. Morfill, H. M. Thomas, B. Steffes, J. Heinlin, S. Karrer, W. Stolz, *Clin. Plasma Med.* **2013**, *1*, 19.

[15] S. J. Kim, T. H. Chung, *Sci. Rep.* **2016**, *6*, 1.

[16] D. B. Graves, *Phys. Plasmas* **2014**, *21*, 080901.

[17] M. G. Kong, G. Kroesen, G. Morfill, T. Nosenko, T. Shimizu, J. van Dijk, J. L. Zimmermann, *New J. Phys.* **2009**, *11*, 115012.

[18] Y. Tian, R. Ma, Q. Zhang, H. Feng, Y. Liang, J. Zhang, J. Fang, *Plasma Processes Polym.* **2015**, *12*, 439.

[19] Y. Xu, Y. Tian, R. Ma, Q. Liu, J. Zhang, *Food Chem.* **2016**, *197*, 436.

[20] J. L. Brisset, B. Benstaali, D. Moussa, J. Fanmoe, E. Njoyim-Tamungang, *Plasma Sources Sci. Technol.* **2011**, *20*, 034021.

[21] J. M. Joslin, J. R. McCall, J. P. Bzdek, D. C. Johnson, B. M., *Plasma Med* **2016**, *6*, 135.

[22] A. Fernandez, E. Noriega, A. Thompson, *Food Microbiol.* **2013**, *33*, 24.

[23] R. Ma, G. Wang, Y. Tian, K. Wang, J. Zhang, J. Fang, *J. Hazard. Mater.* **2015**, *30*, 643.

[24] E. Frías, Y. Iglesias, A. Alvarez-Ordóñez, M. Prieto, M. González-Raurich, M. López, *Food Res. Int.* **2020**, *129*, 108859. https://doi.org/10.1016/j.foodres.2019.108859

[25] G. Kamgang-Youbi, J.-M. Herry, T. Meylheuc, J.-L. Brisset, M.-N. Bellon-Fontaine, A. Doubla, M. Naïtali, *Lett. Appl. Microbiol.* **2009**, *48*, 13.

[26] A. Los, D. Ziuzina, D. Boehm, P. J. Cullen, P. A. Bourke, *Appl. Environ. Microbiol.* **2020**, *86*, 1. https://doi.org/10.1128/AEM.02619-19

[27] J. Guo, K. Huang, X. Wang, C. Lyu, N. Yang, Y. Li, J. Wang, *J. Food Prot.* **2017**, *80*, 225. https://doi.org/10.4315/0362-028X.JFP-16-116

[28] M. J. Traylor, M. J. Pavlovich, S. Karim, P. Hait, Y. Sakiyama, D. S. Clark, D. B. Graves, *J. Phys. D: Appl. Phys.* **2011**, *44*, 472001.

[29] U. K. Ercan, H. Wang, H. F. Ji, G. Fridman, A. D. Brooks, S. G. Joshi, *Plasma Processes Polym.* **2013**, *10*, 544.

[30] J. Shen, Y. Tian, Y. Li, R. Ma, Q. Zhang, J. Zhang, J. Fang, *Sci. Rep.* **2016**, *6*, 28505.

[31] M. J. Traylor, M. J. Pavlovich, S. Karim, P. Hait, Y. Sakiyama, D. S. Clark, D. B. Graves, *J. Phys. D: Appl. Phys.* **2011**, *44*, 47.

[32] C. Smet, M. Govaert, A. Kyrylenko, M. Easdani, J. L. Walsh, J. F. Van Impe, *Front. Microbiol.* **2019**, *10*, 1539.

[33] G. Haghighat, A. Sohrabi, P. Shaibani, C. Van Neste, S. Naicker, T. Thundat, *Environ. Sci.: Water Res. Technol.* **2017**, *3*, 156.

[34] N. Puač, N. Škoro, K. Spasić, S. Živković, M. Milutinović, G. Malović, Z. L. Petrović, *Plasma Processes Polym.* **2018**, *121*, 800. https://doi.org/10.1002/ppap.201700082

[35] M. Naitali, G. Kamgang-Youbi, J. M. Herry, M. N. Bellon-Fontaine, J. L. Brisset, *Appl. Environ. Microbiol.* **2010**, *76*, 7662.

[36] J. X. J. Dai, C. S. Corr, S. B. Ponraj, M. Maniruzzaman, A. T. Ambujakshan, Z. Chen, L. Kviz, R. Lovett, G. D. Rajmohan, D. R. de Celis, M. L. Wright, P. R. Lamb, Y. E. Krasik, D. B. Graves, W. G. Graham, R. d'Agostino, X. Wang, *Plasma Processes Polym.* **2016**, *13*, 306.

[37] S. B. Gupta, H. Bluhm, *IEEE Trans. Plasma Sci.* **2008**, *36*, 1621.

[38] M. J. Pavlovich, H. Chang, Y. Sakiyama, D. S. Clark, D. B. Graves, *J. Phys. D: Appl. Phys.* **2013**, *46*, 145202.

[39] P. Lukes, E. Dolezalova, I. Sisrova, M. Clupek, *Plasma Sources Sci. Technol.* **2014**, *23*, 015019.

[40] R. Zhou, R. Zhou, K. Prasad, Z. Fang, R. Speight, K. Bazaka, K. (Ken) Ostrikov, *Green Chem.* **2018**, *20*, 5276.

[41] D. X. Liu, Z. C. Liu, C. Chen, A. J. Yang, D. Li, M. Z. Rong, H. L. Chen, M. G. Kong, *Sci. Rep.* **2016**, *6*, 23737.

[42] C. Smet, E. Noriega, F. Rosier, J. L. Walsh, V. P. Valdramidis, J. F. Van Impe, *Int. J. Food Microbiol.* **2017**, *240*, 47.

[43] K. Lee, K. H. Paek, W. T. Ju, Y. Lee, *J. Microbiol.* **2006**, *44*, 269.

[44] S. A. Ermolaeva, A. F. Varfolomeev, M. Y. Chernukha, D. S. Yurov, M. M. Vasiliev, A. A. Kaminskaya, M. M. Moisenovich, J. M. Romanova, A. N. Murashev, I. I. Selezneva, T. Shimizu, E. V. Sysolyatina, I. A. Shaginyan, O. F. Petrov, E. I. Mayevsky, V. E. Fortov, G. E. Morfill, B. S. Naroditsky, A. L. Gintsburg, *J. Med. Microbiol.* **2011**, *60*, 75.

[45] R. Thirumdas, A. Kothakota, U. Annapure, K. Siliveru, R. Blundell, R. Gatt, V. P. Valdramidis, *Trends Food Sci. Technol.* **2018**, *77*, 21.

[46] P. Lu, D. Boehm, P. Bourke, P. J. Cullen, *Plasma Processes Polym.* **2017**, *14*, e1600207. https://doi.org/10.1002/ppap.201600207

[47] J. Pan, Y. Li, C. Liu, Y. Tian, S. Yu, K. Wang, J. Zhang, J. Fang, *Plasma Chem. Plasma Process.* **2017**, *27*, 505. https://doi.org/10.1007/s11090-017-9811-0

[48] R. Zhou, R. Zhou, P. Wang, B. Luan, X. Zhang, Z. Fang, Y. Xian, X. Lu, K. Ken Ostrikov, K. Bazaka, *ACS Appl. Mater. Interfaces* **2019**, *11*, 20660.

[49] Y. Akishev, A. Napartovich, M. Grushin, N. Trushkin, N. Dyatko, I. Kochetov, *Food, Biomed. Text. Appl.* **2010**, *121*, 295. https://doi.org/10.1002/9783527630455.ch10

[50] J. Julak, A. Hujacov, V. Scholtz, J. Khun, K. Holada, *Plasma Phy. Rep.* **2018**, *44*, 125.

[51] Y. Sakiyama, D. B. Graves, H.-W. Chang, T. Shimizu, G. E. Morfill, *J. Phys. D: Appl. Phys.* **2012**, *45*, 425201.

[52] Z. Machala, B. Tarabova, D. Sersenova, M. Janda, K. Hensel, *J. Phys. D: Appl. Phys.* **2018**, *2*, 3.

[53] B. M. Penetrante, J. N. Bardsley, M. C. Hsiao, *Jpn. J. Appl. Phys.* **1997**, *36*, 7B.

[54] J. T. Herron, D. S. Green, *Plasma Chem. Plasma Process.* **2001**, *21*, 3.

[55] M. J, V. Martisovits, H. K, *Plasma Chem. Plasma Process.* **2016**, *36*, 767.

[56] M. Capitelli, C. M. Ferreira, B. F. Gordiets, A. I. Osipov, *Plasma Kinetics in Atmospheric Gases*, Splinger, Berlin **2000**.

[57] J. Kruszelnicki, A. M. Lietz, M. J. Kushner, *J. Phys. D: Appl. Phys.* **2019**, *52*, 355207.